Stabilization of the Helical Structure of Y2-Selective Analogues of Neuropeptide Y by Lactam Bridges

Shenggen Yao,[†,‡] Margaret A. Smith-White,[§] Erica K. Potter,[§] and Raymond S. Norton*[,†,‡]

Biomolecular Research Institute, 343 Royal Parade, Parkville, Victoria 3052, Australia, and Prince of Wales Medical Research Institute, Prince of Wales Hospital, Barker Street, Randwick, NSW 2031, Australia

Received November 29, 2001

The importance of helical structure in an analogue of NPY selective for the Y2 receptor, Ac[Leu^{28,31}]NPY$^{24-36}$, has been investigated by introducing a lactam bridge between positions 28 and 32. The resulting analogue, Ac-cyclo$^{28/32}$[Ala^{24},Lys^{28},Leu^{31},Glu^{32}]NPY$^{24-36}$, is a potent Y2-selective agonist. Structural analysis by NMR shows that this analogue forms a helical structure in a 40% trifluoroethanol/water mixture, whereas in water only the region around the lactam bridge (Lys^{28}-Glu^{32}) adopts helical-like structure, with both N- and C-termini being poorly defined. The observation of well-defined helical structure in aqueous TFE contrasts with that reported for a similar analogue, Ac-cyclo$^{28/32}$[Lys^{28},Glu^{32}]NPY$^{25-36}$ (Rist et al. *FEBS Lett.* **1996**, *394*, 169−173), which consisted of a hairpin-like structure that brought the N- and C-termini into proximity. We have therefore determined the structures of this analogue, as well as those of Ac-cyclo$^{28/32}$[Ala^{24},Lys^{28},Leu^{31},Glu^{32}]NPY$^{24-36}$ and Ac-cyclo$^{28/32}$[Ala^{24},Lys^{28},Glu^{32}]-NPY$^{24-36}$, under identical solution conditions (30% TFE/H_2O mixture at 308 K) and find essentially the same helical structure in all three peptides. These findings support the proposal that these Y2-selective analogues adopt a helical structure when bound to the Y2 receptor.

Introduction

Neuropeptide Y (NPY) is a 36-residue, C-terminally amidated polypeptide hormone and neurotransmitter that is active in both the central and peripheral nervous systems. It participates in the regulation of a number of physiological processes, including food intake, blood pressure, circadian rhythms, pain, anxiety, and sexual behavior.[1,2] These activities are mediated by separate receptor subtypes, five of which (Y1, Y2, Y4, Y5, and Y6) have been cloned.[3] NPY is found colocalized with noradrenaline in most sympathetic postganglionic neurons, particularly those innervating the cardiovascular system, where it is released together with noradrenaline during sympathetic nerve stimulation to act at both prejunctional and postjunctional receptors. The prejunctional activity of NPY, mediated by the Y2 receptor, includes inhibition of neurotransmitter release from both sympathetic and parasympathetic nerves. Y2 receptor pharmacology is distinct from that of the other receptor subtypes, since it can be activated by both NPY and shorter carboxy-terminal fragments.[1−3]

NPY has about 50% sequence identity with avian pancreatic polypeptide (PP), for which a crystal structure has been determined.[4] Avian PP formed a symmetrical dimer, with each monomer adopting a hairpin fold consisting of an N-terminal polyPro-like helix (residues 1−8) and a C-terminal α-helix (residues 14−31) linked by a type I β-turn involving residues 9−12. Hydrophobic interactions among side chains from the α-helical regions stabilize the dimer interface. The nonhelical C-terminus (residues 32−36) was flexible and extended away from the bulk of the molecule. The structure of NPY in aqueous solution is not as well defined. Darbon et al.[5] reported that human NPY at pH 3.2 and 37 °C had an avian PP-like fold but did not self-associate. By contrast, in the solution structures of porcine[6] and human[7] NPY at pH 3.2 and 37 °C, the C-terminal segment (residues 11−36 and 13−36, respectively) formed an amphipathic α-helix, the N-terminal region was unstructured, and the molecule was a dimer stabilized by intermolecular interactions between the helices. These NMR studies show that the C-terminal two-thirds of NPY is helical (or has a helical tendency), but the evidence for a hairpin structure of NPY in solution is limited. The fact that such a structure was not observed at low pH[6,7] may be related partly to a pH dependence for interactions between the N- and C-terminal regions.[8,9]

Evidence for self-association of NPY at concentrations typically used in physicochemical studies is unequivocal. Porcine NPY in phosphate buffer at pH 7.4 dimerizes with a K_d of 2 μM, stabilizing the C-terminal α-helix.[10] The monomer retained about 30% α-helix according to circular dichroism (CD), and this was attributed to stabilization of the C-terminal helix by interaction with the N-terminal region. Similar results were obtained by Doughty and Hu,[11] although their CD data implied that monomeric NPY was largely unstructured at biologically relevant concentrations (nanomolar) under physiological conditions. The K_d for self-association of porcine NPY, as monitored by Tyr fluorescence, was relatively independent of pH over the range 2−8, with a mean of 1.6 ± 0.6 μM.[6] In an attempt to reconcile a range of

* To whom correspondence should be addressed. Address: The Walter and Eliza Hall Institute of Medical Research, NMR Laboratory, 381 Royal Parade, Parkville, Victoria 3052, Australia. Phone: +61-3-9903-9650. Fax: +61-3-9903-9655. E-mail: Ray.Norton@wehi.edu.au.
† Biomolecular Research Institute.
‡ Present address: The Walter and Eliza Hall Institute of Medical Research, Parkville, Australia.
§ Prince of Wales Medical Research Institute.

10.1021/jm010543z CCC: $22.00
Published on Web 04/24/2002

experimental observations, Nordmann et al.[12] suggested that NPY exists in a dynamic equilibrium between a small population of "PP-fold" monomer and a "hand-shake" dimer (as described by NMR for porcine and human NPY[6,7]). More recently, a mixture of antiparallel and parallel dimers but no detectable PP-fold was proposed to rationalize NMR relaxation and spin labeling data.[13] In all of these dimer structures, the C-terminal region is α-helical and the dimer interface is stabilized by hydrophobic interactions between these helices.

Although the α-helical structure in the C-terminal half of NPY is stabilized by self-association and possibly interaction with the N-terminal region, as well as by association with membranes,[13] the molecule is largely unstructured at physiological concentrations. Biological data therefore provide the main evidence for the importance of the helical structure and the hairpin fold. Thus, there is ample evidence from studies of NPY structure−function relationships and designed analogues that the N- and C-termini of NPY are in proximity when bound to the Y1 receptor, consistent with a hairpin fold.[1,2,14] The focus of this manuscript is peptides active at the Y2 receptor, for which only the C-terminal region of NPY is needed. Many studies have shown that C-terminal fragments of NPY can indeed form helices[11,15−26] and suggested that the helical structure resembles the receptor-bound structure. Recently, we determined the solution structure and state of association of the C-terminal peptide analogue Ac[Leu^{28,31}]NPY$^{24-36}$, which is a selective agonist for the Y2 receptor.[17,18] Although unstructured in aqueous solution at 5−20 °C, it forms a well-defined helix (encompassing residues 25−35) in 40% trifluoroethanol (TFE)/water at 20 °C.[27] Sedimentation experiments showed that, in contrast to many peptides in aqueous TFE, Ac[Leu^{28,31}]NPY$^{24-36}$ associates to form a trimer or, more likely, a tetramer in 40% TFE, even though it is monomeric in water.

To confirm the importance of helical structure in peptides bound to the Y2 receptor, stabilization in the form of lactam bridges linking residues *i* and *i*+4[28−31] or covalent links between positions *i* and *i*+7[32] could be introduced. Indeed, a series of NPY analogues lacking residues 7−24 but containing *i* to *i*+4 and *i* to *i*+3 lactam bridges in the C-terminal region (residues 25−31) had high affinity for the Y2 receptor, with bridges linking residues 26 and 30 or 27 and 31 showing the tightest binding.[24] The simplest interpretation of these data is that the lactam bridges were stabilizing helical structure at the C-terminus, thereby favoring receptor binding. Around the same time, however, the solution structure of a Y2-selective agonist with a lactam bridge linking positions 28 and 32, Ac-cyclo^{28,32}[Lys^{28},Glu^{32}]-NPY,$^{25-36}$ was reported.[33] Surprisingly, this analogue adopted a hairpin-like structure, bringing the N- and C-termini close together, rather than the anticipated helical structure. The structure−activity data for a series of lactam-bridged variants of this analogue were interpreted subsequently in terms of this hairpin structure, with a correlation being noted between binding affinity and the distances between the N- and C-termini (as predicted from molecular dynamics simulations).[33]

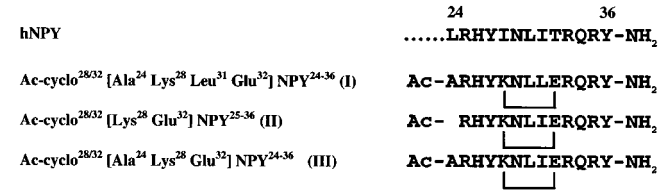

Figure 1. Amino acid sequences of C-terminal NPY analogues used in the present study with a line linking K28 and E32 representing the lactam bridge.

Because we were interested in stabilizing the helical structure of the analogue Ac[Leu^{28,31}]NPY$^{24-36}$, we have introduced a lactam bridge linking positions 28 and 32, exactly as in the analogue described by Rist et al.[33] Our analogue contains an Ala at position 24, a substitution shown to increase the activity of the analogue at the Y2 receptor at the heart in the anesthetised rat.[34] Although this peptide, Ac-cyclo$^{28/32}$[Ala^{24},Lys^{28},Leu^{31},Glu^{32}]NPY$^{24-36}$ (peptide **I**), has limited helical structure in water, it adopts a helical structure in the presence of TFE. Because this result conflicted with expectations based on the structure of Rist et al.,[33] we have also determined the solution structures of their analogue, Ac-cyclo$^{28/32}$[Lys^{28},Glu^{32}]NPY$^{25-36}$ (peptide **II**), as well as Ac-cyclic$^{28/32}$[Ala^{24},Lys^{28},Glu^{32}]NPY$^{24-36}$ (peptide **III**), which has the additional Ala at the N-terminus (Figure 1). Peptides **II** and **III** also differ from **I** in having Ile in position 31, as found in all NPY sequences. All three structures were helical in aqueous TFE, as expected following introduction of a lactam bridge, and all three were active as agonists at the Y2 receptor. Possible reasons for the observation of different structures are considered, and the implications for interpreting structure−activity data for Y2-selective peptides are discussed.

Experimental Section

Sample Preparation and NMR Spectroscopy. NPY was obtained from Calbiochem-Novabiochem (Alexandria, Australia), *N*-acetyl[Leu^{28,31}]NPY$^{24-36}$ from Mimotopes Pty. Ltd. (Clayton, Australia), and lactam analogues **I**−**III** from Auspep (Melbourne, Australia). Peptide purities were ≥95%, and identities were confirmed by mass spectrometry. Peptide content was quantified by reverse-phase HPLC, and molar doses were adjusted accordingly.

NMR samples were prepared by dissolving 3.5−4.0 mg of each peptide in 600 μL (peptide concentration ca. 3 mM) of H_2O containing 10% ^2H_2O, 30% TFE-$^2H_3$, or 40% TFE-$^2H_3$ (by volume). The pH was adjusted to 5.0, measured at room temperature (295 K) without correction for isotope or solvent effects. Spectra were recorded at 298 and 308 K on Bruker AMX-500 and DRX-600 spectrometers. Conventional 2D phase-sensitive TOCSY, NOESY, and DQF-COSY spectra were obtained for each sample using 2048 complex data points in the directly detected dimension (F2) and 512 increments in the F1 dimension, with 64 scans per increment. Spectra were processed using XWINNMR (Bruker AG, Karlsruhe, Germany) with 60° phase-shifted sine-squared window functions applied in both dimensions and were analyzed using XEASY.[35] Spectra were referenced to 2,2-dimethyl-2-silapentane-5-sulfonate via the H_2O signal at 4.77 ppm (298 K)[36] for $H_2O/^2H_2O$ and the residual methylene protons of TFE-$^2H_3$ and at 3.96 ppm for the TFE-$^2H_3$/H_2O mixture,. $^3J_{NHC\alpha H}$ coupling constants were measured from the DQF-COSY spectra as described previously.[37]

Sequence-specific resonance assignments were made using standard procedures.[27,37] The chemical shifts of peptide **I** in

water and 40% TFE at 298 K and peptides **I**−**III** in 30% TFE at 308 K, all at pH 5.0, have been deposited with BioMagResBank (http://www.bmrb.wisc.edu)[38] with accession numbers BMRB-5214, -5215, and -5216.

Structural Constraints and Structure Calculations. Cross-peak volumes measured from a NOESY spectrum recorded at 600 MHz with a mixing time of 250 ms were used to derive upper-bound interproton distance restraints. Conversion from NOE volumes to distance bounds was accomplished using the program CALIBA,[39] with correction for pseudoatoms, and distances were calibrated using the β-methylene protons of Tyr27 and Tyr36. Five predefined classes were employed in CALIBA: (1) intraresidue cross-peaks except those between backbone or β protons, (2) intraresidue and sequential cross-peaks between backbone protons or between backbone and β protons, (3) medium-range (less than five residues apart) cross-peaks between backbone protons or between backbone and β protons, (4) other (i.e., long-range) cross-peaks between backbone protons, and (5) all others. The NOESY cross-peak volumes were considered to be proportional to r^{-6} for classes 2, 3, and 4 and to r^{-4} for classes 1 and 5. After these conversions, a further 0.5 or 1.0 Å was added to distance constraints involving only backbone protons or at least one side chain proton, respectively, to allow for conformational averaging and possible errors in volume integration. Backbone dihedral angle (ϕ) constraints were inferred from $^3J_{NHC}\alpha_H$ coupling constants as follows: $^3J_{NHC}\alpha_H < 5$ Hz, $\phi = -60° \pm 30°$; 5 Hz $\leq {}^3J_{NHC}\alpha_H < 6$ Hz, $\phi = -60° \pm 40°$; $^3J_{NHC}\alpha_H > 8$ Hz, $\phi = -120° \pm 40°$.

Procedures employed in the structure determination were as described previously.[37] In brief, the program DYANA, version 4,[40] was used for the initial evaluation of upper-bound distance restraints in the absence of the lactam bridge. Final structures were generated in X-PLOR[41] starting from a linear template structure and different randomized initial velocity distributions and were subjected to the same simulated annealing protocol. The lactam bridge was included as a distance restraint of 1.30 Å between Lys N^{ζ} and Glu C^{δ}. One hundred structures with the lowest energy were selected from the 400 calculated initially and subjected to further stimulated annealing, in which they were gradually cooled from 300 to 0 K in 20 000 steps and then energy-minimized using 1000 steps of Powell conjugate gradient minimization. For each structure, this procedure was carried out 10 times and the best of these 10 in terms of total energy and NOE energy was selected. Finally, these 100 structures were energy-minimized in the empirical CHARMM force field[42] with a distance-dependent dielectric instead of with explicit water molecules. The best 20 structures based on their stereochemical energies (i.e., the sum of all contributions to the calculated energy excluding the electrostatic term) and NOE energies were chosen for structural analysis. Structural analyses were carried out using the program MOLMOL.[43]

The structures of the three lactam-bridged peptides in 30% TFE/water at 308 K have been deposited with the Protein Data Bank[44] and assigned accession numbers 1D0W (peptide **I**), 1D1E (peptide **II**), and 1D1F (peptide **III**).

Biological Assays. Adult female inbred Wistar rats weighing between 200 and 250 g were anesthetized with sodium pentobarbitone (Nembutal, Boehringer-Ingelhiem; 60 mg/kg ip). The trachea was cannulated, and the animal was artificially ventilated. Temperature was maintained at 35 ± 1 °C, and blood gases were monitored. The left femoral artery was cannulated for continuous recording of arterial blood pressure via a Statham physiological transducer (P23XL) and the femoral vein for administration of drugs. Supplementary doses of sodium pentabarbitone (1:10, diluted in saline) were given as required throughout the experimental period. Subcutaneous needle electrodes recorded the electrocardiogram (ECG), which was displayed on a storage oscilloscope (Gould 1401). The ECG was used to obtain the pulse interval (PI, the time between successive beats of the heart) following processing with Neurolog modules (Digitimer, England NL 200, 303, 601). Both pulse interval and blood pressure (BP) were recorded on a Grass polygraph (79D Grass Instruments).

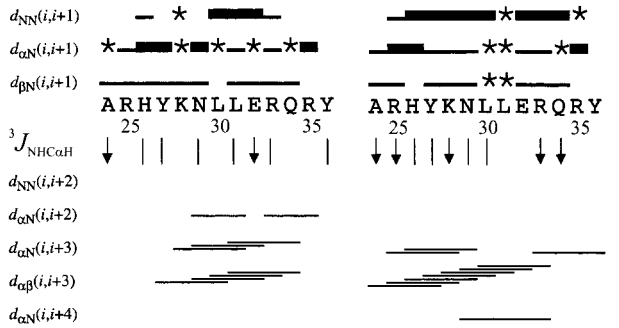

Figure 2. Summary of NMR data for peptide **I** in 90% H_2O/10% ^2H_2O (left) and 40% TFE-$^2H_3$/60% H_2O (right) at 298 K and pH 5.0. Filled bars indicate sequential NOE connectivities, with the heights of the bars reflecting their relative strength (stronger and weaker); a uniform height is used for the medium-range NOE connectivities. An asterisk (*) indicates that the presence of an NOE could not be confirmed unambiguously because of overlap. Values of $^3J_{NHC}\alpha_H$ are indicated by ↓ ($^3J_{NHC}\alpha_H < 6$ Hz), | (6 Hz < $^3J_{NHC}\alpha_H < 8$ Hz), and ↑ ($^3J_{NHC}\alpha_H > 8$ Hz). Residues where $^3J_{NHC}\alpha_H$ could not be measured are left blank.

Both vagus nerves were cut to eliminate vagally mediated reflex effects on the heart following administration of peptides. The cardiac end of the cut right vagus was stimulated using a Grass SD9 isolated square-wave stimulator every 30 s at supramaximal voltage (7.5 V, 2−2.5 Hz for 5 s). The frequency of stimulation increased PI by approximately 100 ms. The maximal inhibition of vagally evoked increase in PI (ΔPI) gave a measure of prejunctional drug activity, while pressor activity obtained from changes in mean arterial pressure (ΔBP) gave a measure of postjunctional drug activity. Previous studies have shown that these parameters produce reliable measures of peptide action at both pre- and postjunctional receptors.[45,46]

Ac[$Leu^{28,31}$]NPY^{24-36} and the three lactam analogues in the dose range 0.5−5 nmol kg^{-1} were injected intravenously in aliquots of 100 μL. Each rat received Ac[$Leu^{28,31}$]NPY^{24-36} and at least two of the lactam analogues; it was not possible for each rat to receive all peptides because of the long duration of evoked inhibitory effects. To compare the effect with the lactam analogues on increase in PI evoked by vagal stimulation, both maximum percent inhibition and time to half recovery were calculated. Dose response histograms were constructed from data generated, and all results are presented as mean ± SEM. Data analysis was performed using SPSS statistical software. An analysis of variance was performed to indicate differences, and where indicated, unpaired Student's *t*-test was used to determine which responses were significantly different from Ac[$Leu^{28,31}$]NPY^{24-36}. *P* values of <0.05 (*) and <0.01 (**) were considered significant.

Results

Structure of Peptide I in H_2O and 40% TFE-$^2H_3$/60% H_2O at 298 K. Experimentally observed sequential and medium-range NOE connectivities, including the $^3J_{NHC}\alpha_H$ coupling constants, are summarized in Figure 2. The distribution of upper-bound distance restraints used in determining the structures in both solvents, together with the backbone rms deviations and angular order parameters (S) for the 20 final structures, is summarized in the Supporting Information (Figure S1). The backbone angular order parameters for peptide **I** were well-defined (S_ϕ, $S_\psi > 0.8$) from Lys^{28} to Arg^{33} in H_2O and from Ala^{24} to Arg^{35} in 40% TFE/H_2O. Figure 3 shows stereoviews of the structure of peptide **I** in H_2O and 40% TFE/H_2O at 298 K. A summary of the struc-

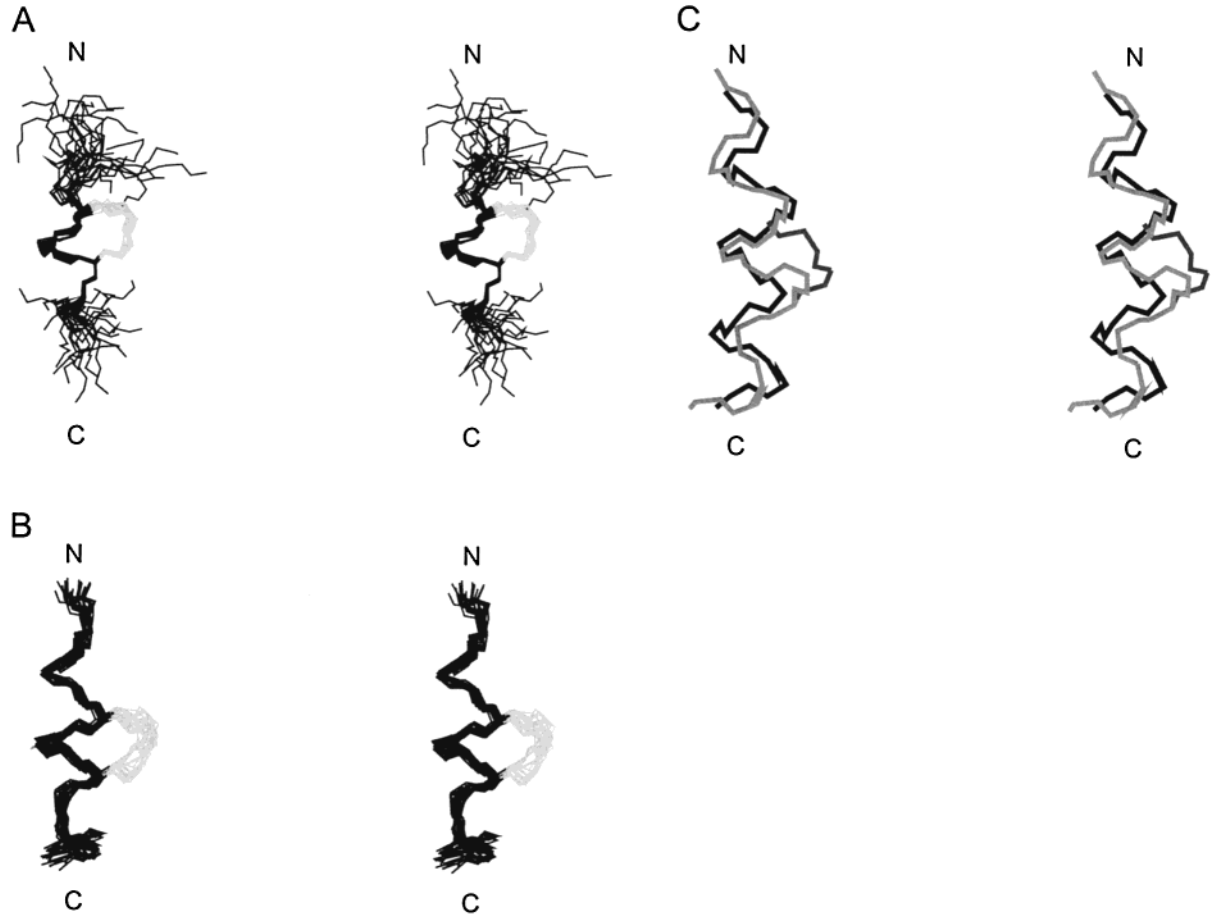

Figure 3. Stereoviews of the backbone atoms of 20 final structures of peptide **I** in 90% H_2O/10% ^2H_2O (A) and 40% TFE-$^2H_3$/60% H_2O (B) at 298 K and pH 5.0. Side chain heavy atoms of Lys^{28} and Glu^{32}, together with the lactam bridge, are shown in gray. In each case the backbone heavy atoms of the 20 final structures are superimposed over their well-defined regions. (C) Superposition of the closest-to-average individual structures of peptide **I** (gray) and Ac[$Leu^{28,31}$]NPY^{24-36} (black). The lactam bridge of peptide **I** is shown in dark-gray. Structures were superimposed over the backbone atoms of all residues.

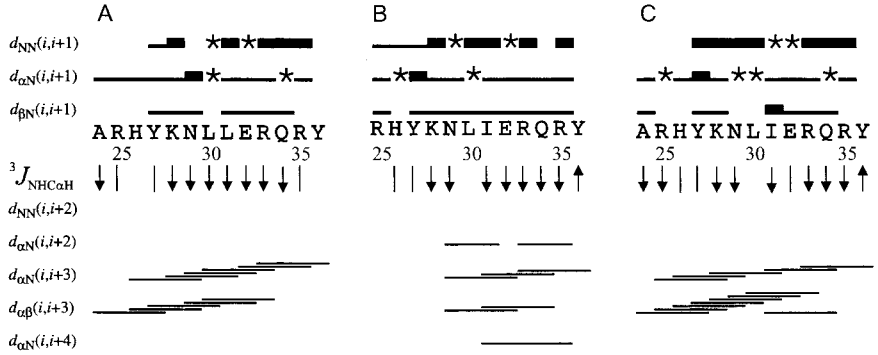

Figure 4. Summary of NMR data for peptides **I** (A), **II** (B), and **III** (C) in 30% TFE-$^2H_3/H_2O$ at 308 K and pH 5.0. Identical notations and symbols to those in Figure 2 were used. Note that the two $d_{\alpha N}(i,i+2)$ NOEs seen for peptide **II** were not evident in spectra of the other two peptides because of spectral overlap. These NOEs are consistent with helical structure but indicative of some distortion from a purely α-helical structure.[51] However, the $d_{\alpha N}(i,i+4)$ NOE spanning this region is indicative of an α-helical structure.[27,51]

tural statistics for these structures is given in the Supporting Information (Table S1).

Structures of Peptides I−III in 30% TFE-$^2H_3$/70% H_2O at 308 K. The sequential and medium-range NOE connectivities, including the $^3J_{NHC}\alpha_H$ coupling constants, are summarized in Figure 4. The presence of numerous $d_{\alpha N}(i,i+3)$, $d_{\alpha N}(i,i+4)$, and $d_{\alpha\beta}(i,i+3)$ NOE connectivities and small $^3J_{NHC}\alpha_H$ coupling constants (<6 Hz) indicate that all three peptides adopt an α-helical-like structure. The structure of peptide **I** was calculated using a total of 124 (55 intraresidue, 42 sequential, and 26 medium) upper-bound distance restraints, excluding those redundant with the covalent geometry (which were eliminated by the program DYANA), and 8 backbone dihedral angle constraints. For peptides **II** and **III**, 130 (56 intraresidue, 43 sequential, and 31 medium) and 114 (53 intraresidue, 36 sequential, and 25 medium) upper-bound distance restraints together with 8 and 9 backbone dihedral angle constraints, respectively, were used. The distribution of these upper-bound distance re-

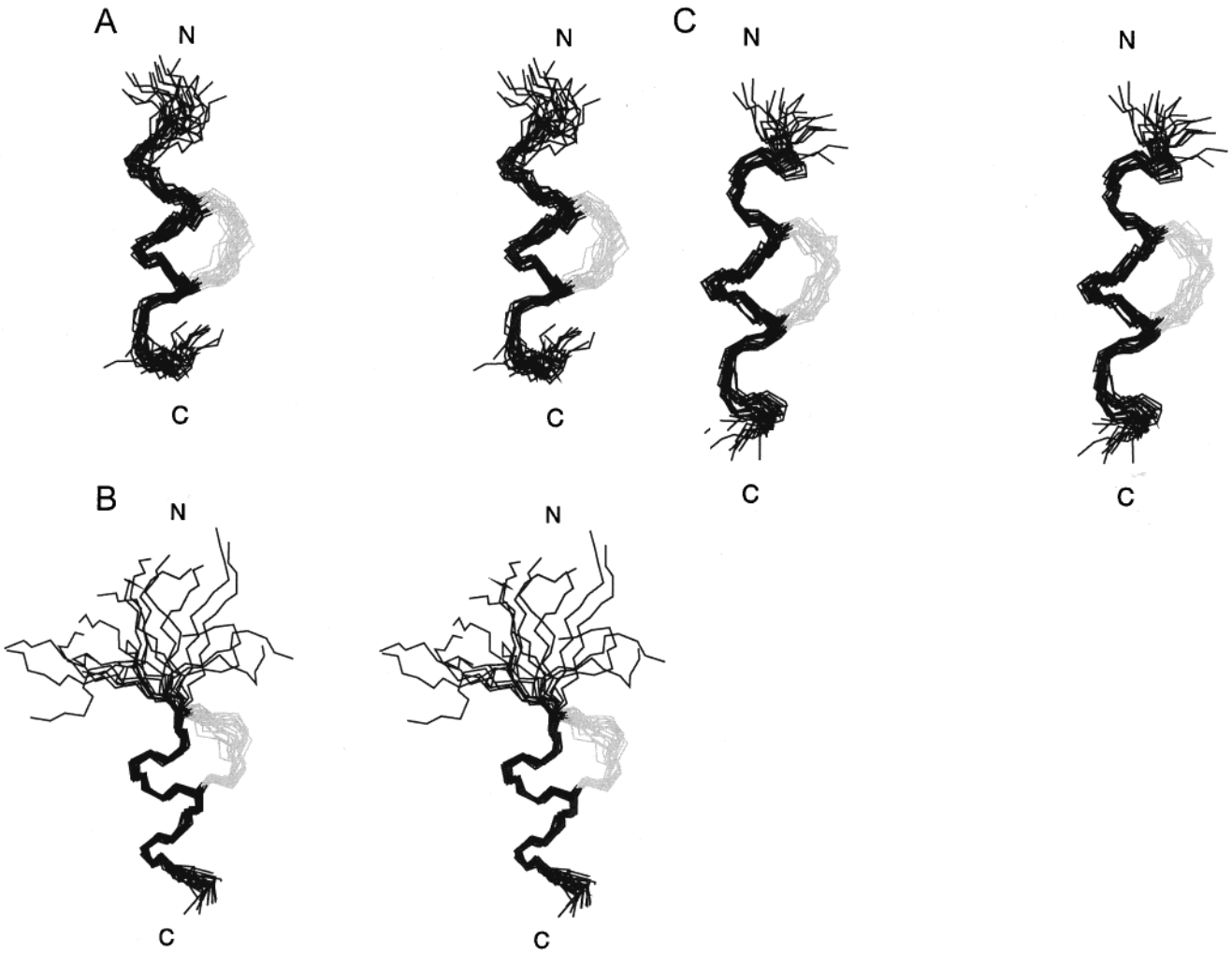

Figure 5. Stereoviews of the backbone atoms of 20 final structures of peptide **I** (A), **II** (B), and **III** (C) in 30% TFE-$^2H_3/H_2O$ at 308 K and pH 5.0 superimposed over backbone heavy atoms of their well-defined regions. The side chain heavy atoms of Lys^{28} and Glu^{32} and the lactam bridge are shown in gray.

straints, together with the backbone rms deviations, angular order parameters (S), and structural statistics for these structures, is given in the Supporting Information (Figure S2 and Table S2).

The backbone angular order parameters (S) of these three sets of final structures indicated that residues Ala^{24} and His^{26}-Arg^{35} of peptide **I**, Lys^{28}-Arg^{35} of peptide **II**, and Arg^{25}-Arg^{35} of peptide **III** were well-defined (S_ϕ, $S_\psi > 0.8$). Stereoviews of the three structures are shown in Figure 5, where the backbone heavy atoms of the 20 final structures are superimposed over their respective well-defined regions. On the basis of ϕ and ψ angles for the angular average structures, these peptides do not form regular α-helices beyond the range of the lactam bridge (positions 28−32). Among those 20 final structures in each case, a number of individual structures form 3_{10}-helix beyond the region of the lactam bridge and several structures have an α-helix extending to Arg^{35}.

Peptide Self-Association. Recently, we investigated the ability of translational diffusion measurements by pulsed field gradient NMR to define the state of self-association of peptides in water and aqueous TFE solutions, using the lactam-bridged peptides described here as a test case.[47] The translational diffusion measurements and sedimentation equilibrium data concurred in showing that all three peptides dimerized in aqueous TFE where they formed helices. By contrast, $Ac[Leu^{28,31}]NPY^{24-36}$ associates to form a trimer or, more likely, a tetramer in 40% TFE, even though it is monomeric in water.[27] It appears that lactam formation inhibits self-association beyond the level of dimers. This could be caused by steric interference, the altered side chain chemistry, or a combination of both. In NOESY spectra of $Ac[Leu^{28,31}]NPY^{24-36}$, some intermolecular NOEs were present, reflecting interactions between monomeric units in the associated form(s). However, intermolecular NOEs were not observed for the lactam-bridged peptides investigated here, presumably reflecting their reduced propensity for self-association.

Minor Species. All three lactam-bridged peptides were ≥95% pure according to analytical reverse-phase HPLC, and their spectra in water gave only a single set of peaks. However, in aqueous TFE, minor peaks representing about 5% of the total were observed from a second form in all three peptides. While it is possible that a minor contaminant was present with chemical shifts essentially identical with the major species in water but not aqueous TFE, we believe these extra peaks in aqueous TFE reflect the presence of a minor conformer. One candidate for this would be structures in which the lactam bridge adopts a cis rather than the

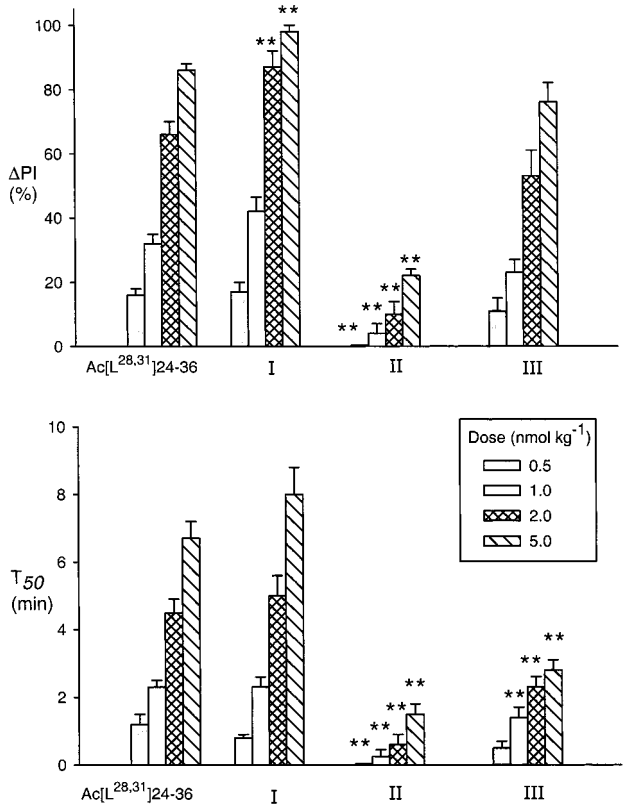

Figure 6. Results from anesthetized rats showing the effect on inhibition of vagal action of Ac[Leu^{28,31}]NPY$^{24-36}$ and lactam analogues **I**−**III**. The histogram shows ΔPI% and T_{50} for peptides in the dose range 0.5−5 nmol kg^{-1}. All peptides attenuated cardiac vagal activity in a dose-dependent manner. The order of potency for evoking an inhibitory effect of vagal action was peptide **I** > Ac[Leu^{28,31}]NPY$^{24-36}$ = peptide **III** > peptide **II**. The time to half recovery of the inhibitory effect was Ac[Leu^{28,31}]NPY$^{24-36}$ = peptide **I** > peptide **III** > peptide **II**. Following ANOVA, comparisons at the same dose levels were made using Student's *t*-test (∗, $P < 0.05$; ∗∗, $P < 0.01$).

trans configuration in the dominant species. Both forms may also exist in water, but the greater flexibility of the structures in water would allow for faster interconversion between them. Stabilization of the helical structure in aqueous TFE could slow this interconversion to the point where separate resonances are observed.

Bioassays. Many of the shortened C-terminal fragments of NPY used as agonists for the Y2 receptor retain activity at other NPY receptors.[48] This study examined Y2-receptor-mediated inhibition of cardiac vagal nerve activity of lactam analogues and compared it to the vagal inhibitory activity evoked by the specific Y_2 agonist[17,18] Ac[Leu^{2831}]NPY$^{24-36}$.

All analogues inhibited cardiac vagal activity in a dose-dependent manner (Figure 6). Ac[Leu^{28,31}]NPY$^{24-36}$ in the dose range 0.5−5 nmol kg^{-1} attenuated the increase in PI evoked by vagal stimulation with a ΔPI ranging from 16 ± 2 to 86 ± 2.5%. ΔPI for peptide **I** ranged from 17 ± 2.5 to 98 ± 2%. The 2 and 5 nmol kg^{-1} doses evoked increases in inhibition compared to Ac[Leu^{28,31}]NPY$^{24-36}$, the increased responses being significantly different ($P < 0.01$). ΔPI for peptide **II** ranged from 0 to 22 ± 2%. The inhibitory effect on cardiac vagal activity evoked by peptide **II** was reduced in comparison to the effects of Ac[Leu^{28,31}]NPY$^{24-36}$. These effects were significantly different for all doses of peptide **II**, $P < 0.01$. ΔPI for peptide **III** ranged from 11 ± 4 to 76 ± 6%. The ΔPI (%) generated from the dose ranges for peptide **III** and Ac[Leu^{28,31}]NPY$^{24-36}$ were not significantly different.

The time to half recovery period for the inhibitory effect on cardiac vagal activity increased in duration with dose (Figure 6). Ac[Leu^{28,31}]NPY$^{24-36}$ in the dose range 0.5−5 nmol kg^{-1} attenuated the increase in PI evoked by vagal stimulation with a T_{50} ranging from 1 ± 0.5 to 8 ± 1.5 min. T_{50} for peptide **I** ranged from 1 to 8 ± 1 min. The evoked responses were not significantly different from those of Ac[Leu^{28,31}]NPY$^{24-36}$. T_{50} for peptide **II** ranged from 0 to 1.5 ± 0.5 min. The time to half recovery period was reduced in comparison to the effects of Ac[Leu^{28,31}]NPY$^{24-36}$. These effects were significantly different for all doses of peptide **II**, $P < 0.01$. T_{50} for peptide **III** ranged from 0.5 to 2.5 ± 0.5 min. The T_{50} values generated from the dose range for peptide **III** and Ac[Leu^{28,31}]NPY$^{24-36}$ were significantly different for all doses, $P < 0.01$.

Ac[Leu^{28,31}]NPY$^{24-36}$ had no effect on blood pressure, as reported previously. Peptides **I**−**III** likewise had no consistent or significant effects on blood pressure.

Discussion

Introduction of a lactam bridge into a 13-residue Y2-selective peptide to produce the analogue Ac-cyclo$^{28/32}$-[Ala^{24},Lys^{28},Leu^{31},Glu^{32}]NPY$^{24-36}$ stabilized the helical structure in the immediate vicinity of the bridge, although in water the N- and C-termini of the peptide remained poorly defined. The addition of TFE stabilized the helical structure throughout the molecule, as expected, although the structure was not as regular an α-helix in aqueous TFE as the unbridged analogue Ac[Leu^{28,31}]NPY$^{24-36}$.[27] To stabilize the helical structure throughout the peptide in the absence of TFE would presumably require the introduction of an additional lactam bridge (possibly overlapping the 28/32 bridge) and/or an *i* to *i* + 7 covalent link.

Because we found a helical structure for Ac-cyclo$^{28/32}$-[Ala^{24},Lys^{28},Leu^{31},Glu^{32}]NPY$^{24-36}$ in aqueous TFE and Rist et al.[33] described a hairpin structure for the closely related peptide Ac-cyclo$^{28/32}$[Lys^{28},Glu^{32}]NPY$^{25-36}$, which differs from our peptide in lacking the N-terminal Ala and having Ile^{31} in place of Leu^{31}, a more detailed comparison was called for. We therefore determined the structures of these two peptides, as well as a third lactam-bridged peptide containing Ala^{24} and Ile^{31}, under solution conditions (30% aqueous TFE, pH 5.0, 308 K) essentially identical to those described by Rist et al.[33]

As shown in Figure 5, all three peptides adopt similar helical structures except for the N-terminus of peptide **II**, which is less well-ordered. The poorer definition of the N-terminus of Ac-cyclo$^{28/32}$[Lys^{28},Glu^{32}]NPY$^{25-36}$ reflects a lack of medium-range NOEs in this region, for example, Ala^{24} to Tyr^{27} and Arg^{25} to Lys^{28}, which were present in peptides **I** and **III** (the former NOE is not possible in peptide **II**, and the latter could not be identified because of peak overlap). Other differences among these three structures reflect minor variations among the three sets of distance and angle constraints used in the structure calculation, which arise mainly from differences in peak overlap in the spectra from

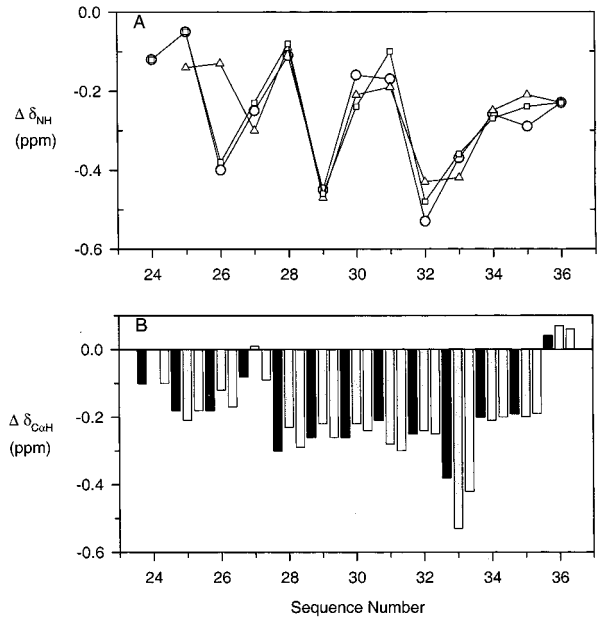

Figure 7. Comparison of ^{1}H chemical shift deviations from random coil values[49] of (A) NH of lactam-bridged peptides **I** (○), **II** (△), and **III** (□) and (B) C$^\alpha$H of **I** (black-filled bar), **II** (gray-filled bar), and **III** (open bar) in 30% TFE-$^2H_3/H_2O$ at 308 K and pH 5.0.

which the restraints were derived. As an independent monitor of solution structure, the ^{1}H chemical shifts of the backbone NH and C$^\alpha$H resonances are very informative.[49] The deviations of these chemical shifts from random coil values are plotted as a function of residue number for all three peptides in Figure 7. The close similarity among the plots for the different peptides beyond Tyr^{27} confirms that their average solution structures are very similar over most of their length. The difference between the NH chemical shifts of Arg^{25} and His^{26} of peptide **II** and those of the other two peptides indicates, however, that the helix does not continue through to the N-terminus in peptide **II** (as also shown in Figure 5). This must result from helix destabilization caused by the absence of Ala^{24}, which is to be expected following truncation of a short isolated helix in solution, but may also reflect the loss of alanine's helix-stabilizing properties. The different C$^\alpha$H chemical shift for Tyr^{27} also points to a difference in the local conformation at this position. Thus, these chemical shift comparisons confirm that residues 25−27 of peptide **II** have a different average conformation from those of the two longer peptides, as implied by the NOE differences and the less well-ordered structure in the N-terminal region of peptide **II**. Importantly, however, they also confirm that the backbone structures for the rest of these three peptides are very similar.

Another valuable monitor of the backbone conformation is the $^3J_{NHC\alpha H}$ coupling constant, which is dependent on the backbone angle ϕ. Plots of these values for peptides **I**−**III**, together with those for Ac[Leu^{28,31}]-NPY$^{24-36}$, which forms a well-defined helix for most of its length,[27] are shown in Figure 8. There is generally good agreement among the values for all four peptides, consistent with similar backbone structures. Values for Leu^{30} of peptides **II** and **III**, both with Ile at position 31, could not be measured accurately because of weak cross-peak intensities in the DQF-COSY spectrum.

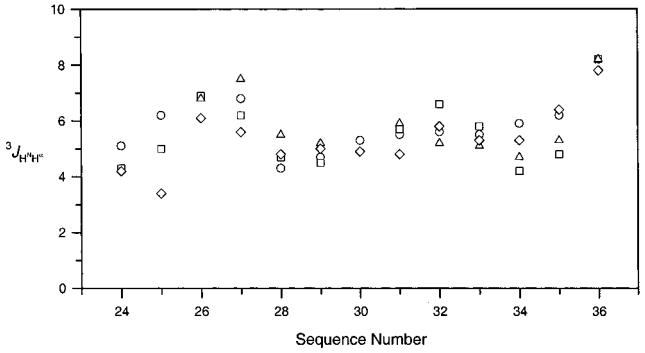

Figure 8. Comparison of vicinal $J_{NH-C\alpha H}$ coupling constants of lactam-bridged peptides **I** (○), **II** (△), and **III** (□) and the linear peptide Ac[Leu^{28,31}]NPY$^{24-36}$ (◇) in 30% TFE-$^2H_3/H_2O$ at 308 K and pH 5.0. All coupling constants were measured from the DQF-COSY spectra as described previously.[37] The $^3J_{NH-C\alpha H}$ coupling constants for Leu^{30} in peptides **II** and **III** were not measured because of the weak NH−C$^\alpha$H cross-peak intensity in the DQF-COSY spectrum. The averaged values for the ϕ angle over the final 20 structures of peptides **II** and **III** are −33° and −48°.

Absence of NOEs between the C- and N-Termini. In an effort to reconcile our structures with the previously published structure of peptide **II**,[33] we searched for possible NOE cross-peaks between the N- and C-termini, as might be expected for a hairpin structure. The low-field quadrants of NOESY spectra of peptides **I** and **II** (Supporting Information, Figure S3) show that NOE cross-peaks between side chains of the C- and N-termini (e.g., the side chains of residues His^{26} and Tyr^{36}) are clearly absent. Furthermore, no $^3J_{NHC\alpha H}$ coupling constants greater than 8 Hz were observed in the central region of the sequence (Figure 4) that might support a hairpin structure.

We have considered whether pH might be a significant factor in the conformation of these peptides. Rist et al. did not specify the pH of their NMR sample, but because their sample was purified by RP-HPLC, it is likely that the pH was low. Given that the peptides are N-terminally acetylated and C-terminally amidated, the only functional group that could change its ionization state between acidic and neutral pH is His^{26}. In the absence of TFE, this residue has a pK_a of 6.0 at 298 K in peptide **I**, so the ionization state at pH 5 would be similar to that at lower pH. The lower pK_a compared with His in small peptides and model compounds (6.4−7.0[50]) presumably reflects its proximity to the positively charged side chain of Arg^{25} and the overall net positive charge on the peptide. NMR spectra were also recorded for peptide **I** in $H_2O/^2H_2O$ at 278 K and in 40% TFE-$^2H_3$ at 308 K. These temperature changes caused no significant structural change as judged by chemical shifts.

Ac[Leu^{28,31}]NPY$^{24-36}$ is a Y2 receptor agonist, equipotent with NPY in attenuating cardiac vagal activity in the anesthetized rat.[34] In the present study, stabilizing the backbone by introduction of a lactam bridge and substituting particular residues in the N-terminal region of the molecule, as in peptide **I**, resulted in an increase in the inhibitory effect on cardiac vagal activity and in time to half recovery of the effect. Peptide **III** differs from peptide **I** in only one residue, Ile^{31}. Leucine in this position was shown previously to be important for inhibitory activity but, more importantly, for in-

creasing the duration of the inhibitory effect on cardiac vagal activity.[34] This is also evident in the lactam analogue, peptide **III**, where inhibitory activity is not significantly different from Ac[Leu^{28,31}]NPY$^{24-36}$ presumably because of the added stability, but the duration of the inhibition has been significantly decreased. Peptide **II** showed the least activity in both cardiac vagal inhibitory effects and time to half recovery. We found previously that shortening the molecule to a 25−36 peptide halved the activity at the Y2 receptor (unpublished data), a result that was unchanged by introduction of the lactam bridge.

The structural data presented in this paper strongly support the notion that the biologically active conformation of the C-terminal region of NPY is helical, as observed for the Y2 agonist Ac[Leu^{28,31}]NPY$^{24-36}$ in aqueous TFE but not in water. It is likely that this helical conformation is induced upon interaction with a biological membrane.[13] Thus, initial contact with biological membranes facilitates receptor interaction not only by reducing the search from a three-dimensional to a two-dimensional problem but also by stabilizing the C-terminal conformation in a structure close to that of the Y2-receptor-bound form. The fact that C-terminal analogues of NPY retain potent activity at the Y2 receptor following introduction of a lactam bridge is entirely consistent with this view, and the structural data presented here have confirmed that the structures of these lactam analogues are indeed helical. Further modification of the C-terminal sequence to stabilize a helical conformation, or even the introduction of nonpeptidic helix initiators at the N-terminus, can now be pursued.

Acknowledgment. We thank Dr. Bob Miller for many helpful discussions. This work was supported in part by the Cooperative Research Centre for Biopharmaceutical Research.

Supporting Information Available: Two figures showing summaries of structural parameters (NOE distribution, rms deviations, angular order parameters) for peptides in water and aqueous TFE, one figure showing the downfield regions of NOESY spectra of peptides **I** and **II**, and two tables summarizing structural statistics for all structures presented in this paper. This material is available free of charge via the Internet at http://pubs.acs.org.

References

(1) Colmers, W. F., Wahlestedt, C., Eds. *The Biology of Neuropeptide Y and Related Peptides*; Humana: Totowa, NJ, 1993.
(2) Grundemar, L.; Håkanson, R. Neuropeptide Y Effector Systems: Perspectives for Drug Development. *Trends Pharmacol. Sci.* **1994**, *15*, 153−158.
(3) Michel, M. C.; Beck-Sickinger, A.; Cox, H.; Doods, H. N.; Herzog, H.; Larhammar, D.; Quirion, R.; Schwartz, T.; Westfall, T. XVI. International Union of Pharmacology Recommendations for the Nomenclature of Neuropeptide Y, Peptide YY, and Pancreatic Polypeptide Receptors. *Pharmacol. Rev.* **1998**, *50*, 143−150.
(4) Blundell, T. L.; Pitts, J. E.; Tickle, I. J.; Wood, S. P.; Wu, C.-W. X-ray Analysis (1.4 Å resolution) of Avian Pancreatic Polypeptide: Small Globular Protein Hormone. *Proc. Natl. Acad. Sci. U.S.A.* **1981**, *78*, 4175−4179.
(5) Darbon, H.; Bernassau, J.-M.; Deleuze, C.; Chenu, J.; Roussel, A.; Cambillau, C. Solution Conformation of Human Neuropeptide Y by ^{1}H Nuclear Magnetic Resonance and Restrained Molecular Dynamics. *Eur. J. Biochem.* **1992**, *209*, 765−771.
(6) Cowley, D. J.; Hoflack, J. M.; Pelton, J. T.; Saudek, V. Structure of Neuropeptide Y Dimer in Solution. *Eur. J. Biochem.* **1992**, *205*, 1099−1106.
(7) Monks, S. A.; Karagianis, G.; Howlett, G. J.; Norton, R. S. Solution Structure of Human Neuropeptide Y. *J. Biomol. NMR* **1996**, *8*, 379−390.
(8) Krstenansky, J. L.; Buck, S. H. The Synthesis, Physical Characterization and Receptor-Binding Affinity of Neuropeptide Y (NPY). *Neuropeptides* **1987**, *10*, 77−85.
(9) Saudek, V.; Pelton, J. T. Sequence-specific ^{1}H NMR Assignment and Secondary Structure of Neuropeptide-Y in Aqueous-Solution. *Biochemistry* **1990**, *29*, 4509−4515.
(10) Minakata, H.; Taylor, J. W.; Walker, M. W.; Miller, R. J.; Kaiser, E. T. Characterization of Amphiphilic Secondary Structures in Neuropeptide Y through the Design, Synthesis, and Study of Model Peptides. *J. Biol. Chem.* **1989**, *264*, 7907−7913.
(11) Doughty, M. B.; Hu, L. The Contribution of Helical Potential to the in Vitro Receptor Binding Activity of a Neuropeptide Y N-Terminal Deletion Fragment. *Biopolymers* **1993**, *33*, 1195−1206.
(12) Nordmann, A.; Blommers, M. J. J.; Fretz, H.; Arvinte, T.; Drake, A. F. Aspects of the Molecular Structure and Dynamics of Neuropeptide Y. *Eur. J. Biochem.* **1999**, *261*, 216−226.
(13) Bader, R.; Bettio, A.; Beck-Sickinger, A. G.; Zerbe, O. Structure and Dynamics of Micelle-Bound Neuropeptide Y: Comparison with Unligated NPY and Implications for Receptor Selection. *J. Mol. Biol.* **2001**, *305*, 307−329.
(14) Beck-Sickinger, A. G. In *Neuropeptide Y and Drug Development*; Grundemar, L., Bloom, S. R, Eds.; Academic Press: San Diego, CA, 1997; pp 107−126..
(15) Murase, S.; Yumoto, N.; Petukhov, M. G.; Yoshikawa, S. Acylation of the Alpha-amino Group in Neuropeptide Y(12−36) Increases Binding Affinity for the Y2 Receptor. *J. Biochem. (Tokyo)* **1996**, *119*, 37−41.
(16) Boublik, J.; Scott, N.; Taulane, J.; Goodman, M.; Brown, M.; Rivier, J. E. Neuropeptide-Y and Neuropeptide Y18−36− Structural and Biological Characterization. *Int. J. Pept. Protein Res.* **1989**, *33*, 11−15.
(17) Barden, J. A.; Cuthbertson, R. M.; Potter, E. K.; Selbie, L. A.; Tseng, A. Stabilized Structure of the Presynaptic (Y2) Receptor-Specific Neuropeptide-Y Analog N-acetyl[Leu-28,Leu-31] NPY-(24−36). *Biochim. Biophys. Acta* **1994**, *1206*, 191−196.
(18) Potter, E. K.; Barden, J. A.; McCloskey, M. J. D.; Selbie, L. A.; Tseng, A.; Herzog, H.; Shine J. A Novel Neuropeptide-Y Analog, N-Acetyl[Leu(28),Leu(31)] Neuropeptide Y(24−36), with Functional Specificity for the Presynaptic (Y2) Receptor. *Eur. J. Pharmacol.* **1994**, *267*, 253−262.
(19) Arvidsson, K.; Jarvet, J.; Allard, P.; Ehrenberg, A. Solution Structure by ^{1}H and Dynamics by Natural-Abundance ^{13}C NMR of a Receptor Recognizing Peptide Derived from a C-Terminal Fragment of Neuropeptide-Y. *J. Biomol. NMR* **1994**, *4*, 653−672
(20) Barden, J. A. Structure of Prejunctional Receptor-Binding Analog of Human Neuropeptide-Y Dimer ANA-NPY. *Biochem. Biophys. Res. Commun.* **1995**, *215*, 264−271.
(21) Chu, S. S.; Velde, D. V.; Shobe, D.; Balse, P.; Doughty, M. B. Conformational Properties of the Proline Region of Porcine Neuropeptide-Y by CD and ^{1}H-NMR Spectroscopy. *Biopolymers* **1995**, *35*, 583−593.
(22) Leban, J. J.; Heyer, D.; Landavazo, A.; Matthews, J.; Aulabaugh, A.; Danniels, A. J. Novel Modified Carboxy-Terminal Fragments of Neuropeptide-Y with High-Affinity for Y2-Type Receptors and Potent Functional Antagonism at Y1-Type Receptor. *J. Med. Chem.* **1995**, *38*, 1150−1157.
(23) Gurrath, M.; Bisello, A.; Bottazzo, K.; Chung, C.-W.; Mammi, S.; Peggion, E. Conformational Analysis of Neuropeptide Y Segments by CD, NMR Spectroscopy and Restrained Molecular Dynamics. *J. Pept. Sci.* **1996**, *2*, 176−193.
(24) Kirby, D. A.; Britton, K. T.; Aubert, M. L.; Rivier, J. E. Identification of High-Potency Neuropeptide Y Analogues through Systematic Lactamization. *J. Med. Chem.* **1997**, *40*, 210−215.
(25) Labelle, M.; St-Pierre, S.; Savard, R.; Boulanger, Y. Solution Structure of Neuropeptide Tyrosine 13−36, a Y2 Receptor Agonist, As Determined by NMR. *Eur. J. Biochem.* **1997**, *246*, 780−785.
(26) Uegaki, K.; Murase, S.; Nemoto, N.; Kobayashi, Y.; Yoshikawa, S.; Yumoto, N. Effects of Covalent Dimerization on the Structure and Function of the Carboxy-Terminal Fragment of Neuropeptide Y. *Biochem. Biophys. Res. Commun.* **1997**, *241*, 737−743.
(27) Barnham, K. J.; Catalfamo, F.; Pallaghy, P. K.; Howlett, G. J.; Norton, R. S. Helical Structure and Self-Association in a 13 Residue Neuropeptide Y Y2 Receptor Agonist: Relationship to Biological Activity. *Biochim. Biophys. Acta* **1999**, *1435*, 127−137.
(28) Felix, A. M.; Heimer, E. P.; Wang, C.-T.; Lambros, T. J.; Fournier, A.; Mowles, T. F.; Maines, S.; Campbell, R. M.; Wegrzynski, B. B.; Toome, V.; Fry, D.; Madison, V. S. Synthesis, Biological Activity and Conformational Analysis of Cyclic GRF Analogs. *Int. J. Pept. Protein Res.* **1988**, *32*, 441−454.
(29) Osapay, G.; Taylor, J. W. Multicyclic Polypeptide Model Compounds. 2. Synthesis and Conformational Properties of a Highly Alpha-Helical Uncosapeptide Constrained by 3 Side-Chain to Side-Chain Lactam Bridges. *J. Am. Chem. Soc.* **1992**, *114*, 6966−6973.

(30) Houston, M. E.; Gannon, C. L.; Kay, C. M.; Hodges, R. S. Lactam Bridge Stabilization of α-Helical Peptides: Ring Size, Orientation and Positional Effects. *J. Pept. Sci.* **1995**, *1*, 274−282.
(31) Houston, M. E.. Jr.; Campbell, A. P.; Lix, B.; Kay, C. M.; Sykes, B. D.; Hodges, R. S. Lactam Bridge Stabilization of α-Helices: The Role of Hydrophobicity in Controlling Dimeric versus Monomeric α-Helices. *Biochemistry* **1996**, *35*, 10041−10050.
(32) Phelan, J. C.; Skelton, N. J.; Braisted, A. C.; McDowell, R. S. A General Method for Constraining Short Peptides to an α-Helical Conformation. *J. Am. Chem. Soc.* **1997**, *119*, 455−460.
(33) Rist, B.; Zerbe, O.; Ingenhoven, N.; Scapozza, L.; Peers, C.; Vaughan, P. F. T.; McDonald, R. L.; Wieland, H. A.; Beck-Sickinger, A. G. Modified, Cyclic Dodecapeptide Analog of Neuropeptide Y is the Smallest Full Agonist at the Human Y_2 Receptor. *FEBS Lett.* **1996**, *394*, 169−173.
(34) Smith-White, M. A.; Potter, E. K. Structure−Activity Analysis of N-Acetyl[Leu(28,31)] NPY 24−36: A Potent Neuropeptide Y Y2 Receptor Agonist. *Neuropeptides* **1999** *33*, 526−533.
(35) Bartels, C.; Xia, T.-H.; Güntert, P.; Wüthrich, K. The Program XEASY for Computer-Supported NMR Spectral Analysis of Biological Macromolecules. *J. Biomol. NMR* **1995**, *6*, 1−10.
(36) Wishart, D. S.; Bigam, C. G.; Yao, J.; Abildgaard, F.; Dyson, J. E.; Oldfield, E.; Markley, J. L.; Sykes, B. D. ^{1}H, ^{13}C and ^{15}N Chemical Shift Referencing in Biomolecular NMR. *J. Biomol. NMR* **1995**, *6*, 135−140.
(37) Barnham, K. J.; Monks, S. A.; Hinds, M. G.; Azad, A. A.; Norton, R. S. Solution Structure of a Polypeptide from the N Terminus of the HIV Protein Nef. *Biochemistry* **1997**, *36*, 5970−5980.
(38) Seavey, B. R.; Farr, E. A.; Westler, W. M.; Markley, J. L. A Relational Database for Sequence-Specific Protein NMR Data. *J. Biomol. NMR* **1991**, *1*, 217−236.
(39) Güntert, P.; Braun, W.; Wüthrich, K. Efficient Computation of Three-Dimensional Protein Structures in Solution from Nuclear Magnetic Resonance Data Using the Program DIANA and the Supporting Programs CALIBA, HABAS and GLOMSA. *J. Mol. Biol.* **1991**, *217*, 517−530.
(40) Güntert, P.; Mumenthaler, C.; Wüthrich, K. Torsion Angle Dynamics for NMR Structure Calculation with the New Program DYANA. *J. Mol. Biol.* **1997**, *273*, 283−298.
(41) Brünger, A. T. *X-PLOR: A System for X-ray Crystallography and NMR*, version 3.1; Yale University: New Haven, CT, 1992.
(42) Brooks, B. B.; Bruccoleri, R. E.; Olafson, B. D.; States, D. J.; Swaminathan, S.; Karplus, M. CHARMM: A Program for Macromolecular Energy Minimization and Danamics Calculations. *J. Comput. Chem.* **1983**, *4*, 187−217.
(43) Koradi, R.; Billeter, M.; Wüthrich, K. MOLMOL: A Program for Display and Analysis of Macromolecular Structure. *J. Mol. Graphics* **1996**, *14*, 51−55.
(44) Bernstein, F. C.; Koetzle, T. F.; Williams, G. J. B.; Meyer, E. F.; Brice, M. D.; Rodgers, J. R.; Kennard, O.; Shimanouchi, T.; Tasumi, M. The Protein Data Bank: A Computer-Based Archival File for Macromolecular Structures. *J. Mol. Biol.* **1977**, *112*, 535−542.
(45) Potter, E. K. Neuropeptide Y as an Autonomic Transmitter (Review). In *International Encyclopedia of Pharmacology and Therapeutics; Novel Peripheral Transmitters*; Bell, C., Ed.; Pergamon Press: New York, 1991; pp 81−112.
(46) Potter, E. K.; Mitchell, L.; McCloskey, M. J. D.; Tseng, A.; Goodman, A. E.; Shine, J.; McCloskey, D. I. Prejunctional and Postjunctional Actions of Neuropeptide-Y and Related Peptides. *Regul. Pept.* **1989**, *25*, 167−177.
(47) Yao, S.; Howlett, G. J.; Norton, R. S. Peptide Self-Association in Aqueous Trifluoroethanol Monitored by Pulsed Field Gradient NMR Diffusion Measurements. *J. Biomol. NMR* **2000**, *16*, 109−119.
(48) Smith-White, M.; Moriarty, M. J.; Potter, E. K. A Comparison of Actions of Neuropeptide Y (NPY) Agonists and Antagonists at NPY Y1 and Y2 Receptors in Anaesthetized Rats. *Neuropeptides* **1998**, *32*, 109−118.
(49) Wishart, D. S.; Sykes, B. D. Chemical Shifts as a Tool for Structure Determination. *Methods Enzymol.* **1994**, *239*, 363−392.
(50) Gooley, P. R.; Blunt, J. W.; Beress, L.; Norton, R. S. Effects of pH and Temperature on Cardioactive Polypeptides from Sea Anemones: A ^{1}H-NMR Study. *Biopolymers* **1988**, *27*, 1143−1157.
(51) Wüthrich, K. *NMR of Proteins and Nucleic Acids*; John Wiley and Sons: New York, 1986.

JM010543Z